Expanding the RGB Color Gamut by the Fourth Color

Abstract

The natural world perceived by the human eye cannot be fully represented by light-emitting diode (LED) displays, primarily because natural light sources, such as sunlight, typically have a continuous spectrum covering a wide range of wavelengths from ultraviolet to infrared. In contrast, LED displays typically rely on red, green, and blue (RGB) LEDs combined using the additive color principle to produce visible light. These LEDs emit discrete narrowband spectra, resulting in a limited color gamut, a color range that a system can present. This gamut is often constrained to follow specific standards such as standard RGB (sRGB), AdobeRGB, or DCI-P3, which fail to encompass the full range of colors found in nature. For instance, some deep blues or vivid greens cannot be accurately reproduced on standard displays. In this project, we propose extending the display color gamut by adding a new color to LED displays' commonly used RGB. To achieve this, we utilized calculations to model the response of human cone cells, photoreceptors responsible for color perception, to various wavelengths of light. Through linear combinations, we compared the range of human-visible colors with the RGB gamut. Our calculations revealed that, without considering brightness effects, standard RGB LED displays can only reproduce approximately 52% of the colors within the human-visible spectrum. By examining the entire visible light spectrum, we identified the optimal additional wavelength for expanding the LED gamut: 400 nm violet. The inclusion of this wavelength increases the RGB color gamut by around 38%, enabling the present of approximately 72% of the colors visible to the human eye. In practical applications, a circuit system with a Digital to analog converter **(**DAC) and NPN transistors was built to control the current through LEDs, and a translucent plastic cover was used to combine the LEDs. In the future work, we are going to add more LEDs with different wavelengths to further expand the color gamut.

Introduction

Throughout the history of humanity's efforts to represent the colors of the natural world using electronic devices, continuous technological advancements have significantly transformed the way colors are perceived and expressed. However, it is still not possible to display all the colors that humans can perceive in nature on the monitors. The fundamental reason lies in the biological mechanism of human color perception. Humans perceive color through the cone cells, short-wavelength cone cells (S-cones), medium-wavelength cone cells (M-cones), and long-wavelength cone cells (L-cones), in the retina. Cones have different responses (Fig. 1) to light of different wavelengths. In nature, a continuous spectrum, such as sunlight, stimulates cones across all possible combinations, producing the rich variety of colors humans can perceive. However, electronic displays rely on combinations of usually red, green, and blue (RGB) LEDs to reproduce colors. This approach, based on the principle of additive color, provides only a limited subset of the responses that cone cells can generate, restricting the range of colors monitors can display.

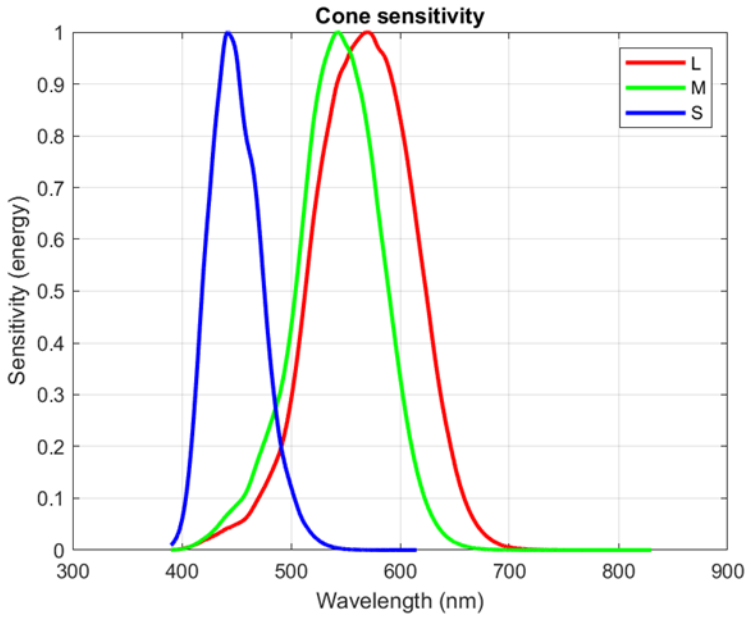

Fig. 1. The responses of L-cones, M-cones, and S-cones to light with different wavelengths. The *x*-axis represents the light wavelength, and the *y*-axis is the normalized cones' responses.

These limitations in replicating natural colors did not deter technological innovation. In the early 20th century, black-and-white televisions [1, 2], the first generation of electronic displays,

presented visual information solely through brightness contrasts. While this technology ushered in a new era of visual entertainment, it fell short of satisfying the human desire for a faithful reproduction of the colorful world. The subsequent advent of color television [2, 3] marked a significant milestone, utilizing the three primary colors, RGB, to synthesize and reproduce colors, allowing electronic devices to render visuals closer to reality for the first time. With the advancement of technology, the sRGB color space [4, 5, 6] emerged as the dominant standard for display devices. Despite its significant advantages in terms of cost and compatibility, sRGB's color gamut remains limited, covering only a fraction of the visible spectrum perceived by the human eye. To address this limitation, subsequent developments introduced wider-gamut standards such as Adobe RGB [6, 7], ProPhoto RGB [6, 8], and DCI-P3 [9] because the LEDs they used have different wavelengths. These expanded gamut standards greatly enhanced the color performance of electronic devices, driving transformations in industries such as photography, cinema, and design. However, even the most advanced wide-gamut display technologies still fall short of covering the entirety of human-visible colors, particularly in rendering certain extreme hues such as deep purples or saturated greens [10].

Against this backdrop, this project aims to explore methods for further expanding the color gamut by proposing a novel four-primary LED system. Traditional three-primary LED systems synthesize colors using RGB light sources, but their gamut is constrained by the spectral response of the cone cells to these three wavelengths. To overcome this limitation, we propose adding a violet LED to the existing RGB system to cover shorter wavelengths in the violet region, significantly expanding the color gamut. This design optimizes the spectral response to the short-wavelength cone cells (S-cones), enabling display devices to reproduce a wider variety of natural colors.

The objective of this study is to design, implement, and validate the performance of the four-primary LED system. We will review the technical history and challenges of color gamut expansion, analyze the theoretical improvements in color coverage offered by the four-primary approach, and evaluate its practical performance through experiments. This breakthrough not only advances display technology but also provides novel solutions for applications requiring high color fidelity, such as medical imaging, art restoration, and premium displays. Ultimately, it

drives progress in color science and display technology, pushing the boundaries of what is visually achievable.

Result

Theory and Calculation

To quantify and analyze the range of colors perceivable by the human eye and the proportion of these colors that the existing RGB gamut can simulate, we constructed a three-dimensional coordinate system with *L*, *M*, and *S* as the axes. This system represents the human-visible color gamut based on the relationship between light wavelengths and the responses of L-cones, M-cones, and S-cones (LMS) [11, 12], and it was used to compare the distribution of the RGB gamut. Specifically, we utilized wavelength data from ultra-bright 5 mm LEDs provided by Adafruit, with peak wavelengths of 465 nm (blue) [13], 520 nm (green) [14], and 640 nm (red) [15], which correspond to the principal colors in the RGB gamut.

To facilitate comparison, we normalized the luminance of all data points and projected them onto the $L + M + S = 1$ plane, as constant brightness. This approach is similar to the representation method used in the Commission Internationale de l'Éclairage (CIE) chromaticity diagram [10], making it easier to compare the size and coverage of different gamuts intuitively.

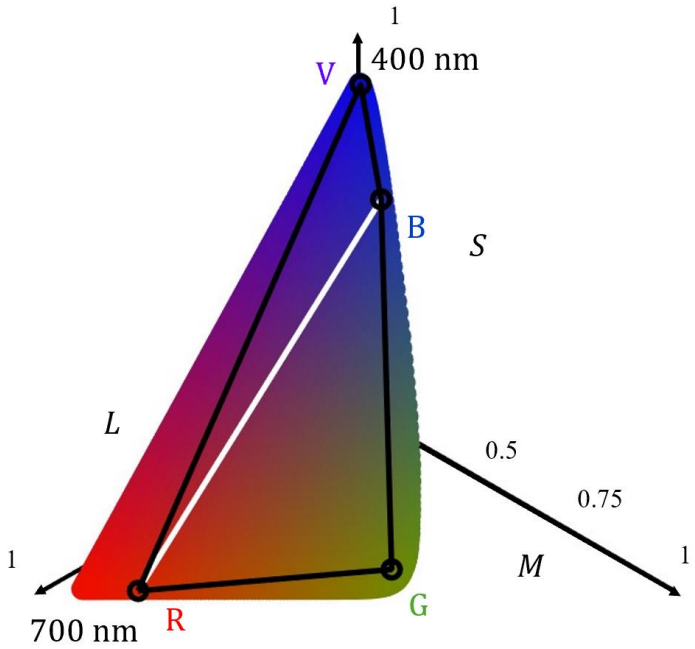

Fig. 2. The colored area represents the human-visible color gamut; the white boundary encloses the RGB gamut; the black boundary encloses the RGBV gamut. The *L*-axis, *M*-axis, and *S*-axis represent the normalized responses of L-cones, M-cones, and S-cones, respectively. R, G, B, and V refers to the LEDs used.

Based on Fig.2, we can intuitively observe that the color gamut formed by the RGB primaries occupies only a portion of the area encompassed by the human-visible spectrum. According to program-based area calculations, this amount is approximately 52%. This indicates that the current RGB gamut cannot fully cover the entire human-visible color gamut. Given that the human-visible color gamut significantly exceeds the RGB gamut, we conclude that there is considerable potential for improvement in color simulation by expanding the RGB gamut to include more colors perceivable by the human eye.

To further explore the possibility of gamut expansion, we considered increasing the gamut range by introducing a fourth primary color. To quantify the effect of this expansion, we systematically traversed the visible spectrum from the shortest to the longest wavelength, using each monochromatic light wavelength as the fourth primary color in combination with the RGB primaries. By calculating the area of the color gamut formed by the four primaries, we compared it to the area of the RGB gamut. Specifically, we defined a ratio p to represent the proportion of the four-primary color gamut area relative to the RGB gamut area. This ratio provides a measure of the effectiveness of gamut expansion by introducing a fourth primary color.

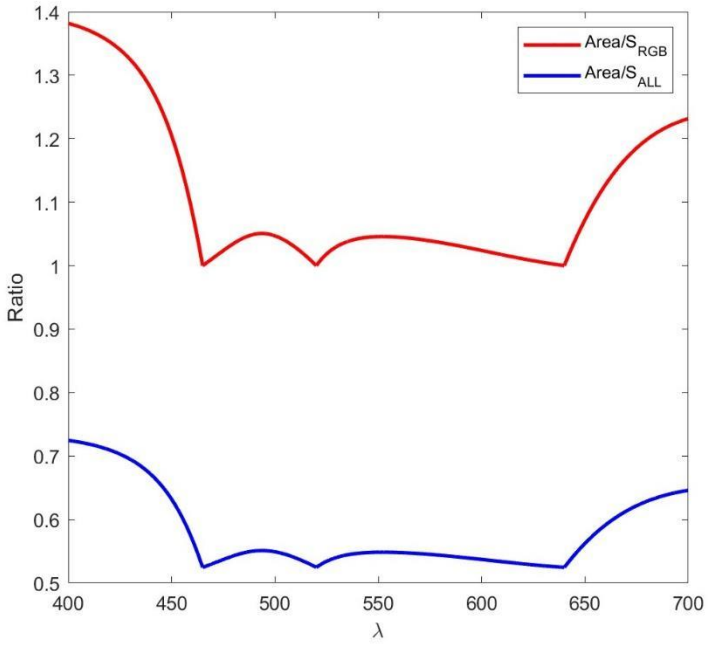

Fig. 3. The *x*-axis represents the wavelength of the fourth primary color, and the *y*-axis represents the ratio. The red line indicates the ratio p of the four-primary color gamut area to the RGB color gamut area, while the blue line also represents the ratio of the four-primary color gamut area to the human-visible color gamut area.

In Fig. 3, we observe that at the wavelengths of 465 nm, 520 nm, and 640 nm, *p* equals 1, indicating that the color gamut area does not expand at these wavelengths. Since these wavelengths correspond to the three RGB primary colors, the fourth primary color overlaps with these colors and the color gamut area does not increase. This is the expected result of our theoretical calculation. Through this validation step, we initially determined the accuracy of the program. Additionally, we found that *p* reaches a local maximum at approximately 400 nm (in the violet range), 500 nm (in the green range), and 700 nm (in the deep red range). The color gamut area enclosed by the four primaries shows a significant increase compared to the RGB gamut area. Particularly at 400 nm, the color gamut area formed by the four primaries reaches its maximum, showing that violet light contributes the most to expanding the color gamut. Therefore, we decided to select a violet LED as the fourth primary color for the experiment to extend the color gamut further.

In practice, we chose the 400 nm violet 5 mm LED from Adafruit [16] as the fourth primary color. This choice resulted in a 38.18% increase in the color gamut area compared to the color gamut formed by the RGB primaries alone, representing approximately 72% of the human-visible spectrum, while the RGB gamut only covers around 52%. This result demonstrates that introducing a violet LED can significantly expand the color gamut, especially in the violet light region, allowing the four-primary color combination to simulate colors that are not achievable with the RGB gamut.

Application

Through the analysis and calculations conducted in this study, we conclude that using a violet LED as the fourth primary color can significantly extend the RGB color gamut, especially in the violet light region. The combination of four primary colors can cover more visible colors, approaching the actual color gamut range perceived by the human eye. Therefore, we designed a circuit to verify theoretical findings experimentally.

To precisely control the brightness of the LEDs in the experiment, this study utilizes the Arduino Mega 2560 [17], the LEDs, a DAC [18], NPN transistors [19], and fixed resistors [20], forming the circuit as Fig. 4.

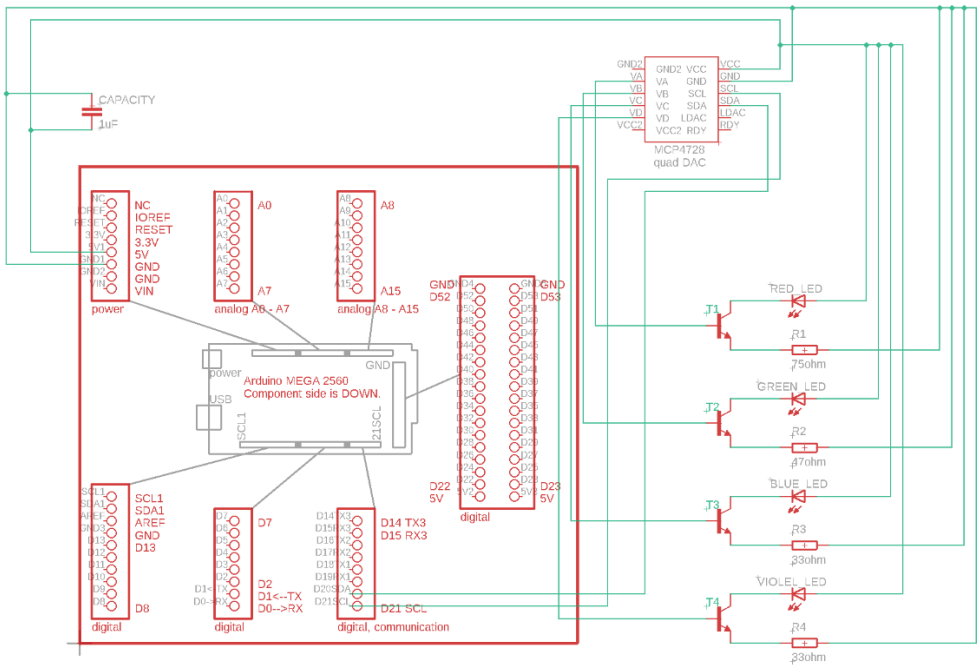

Fig. 4. Circuit in the application.

Notably, LEDs exhibit significant nonlinear working characteristics [21] when they are connected to the circuit individually. When the forward voltage of the LED approaches its threshold voltage, it enters a nonlinear working region, where the current-voltage relationship becomes steeply exponential. A small change in voltage results in a substantial increase in current due to the voltage clamping effect. Therefore, by adjusting the base voltage of the DAC and using a series resistor to limit the current, we can not only precisely control the brightness of the LED but also prevent damage to the LED due to excessive current. However, since the current output capacity of the DAC is limited to only 12 mA, this is insufficient to meet the maximum continuous operating current requirements of the LED used in this study. To address this, we introduce an NPN transistor in the circuit as a current amplifier. By controlling its base voltage with the DAC, the NPN transistor can effectively amplify the current flowing through the LED [22], and the current can be adjusted by the DAC voltage outputs. This allows the system to precisely control the brightness of the LED within its normal operating voltage range. And We found the resistors of appropriate values, via calculation and experiments, to ensure that the current through each LED is close to their maximum current when the DAC outputs the maximum voltage (Tab. 1 and Fig. 5).

	Range of Voltage (mV)	**Range of Current (mA)**	**Matching Resistor (ohm)**
Red	0 ~ 1.96	0 ~ 29.0	75
Green	0 ~ 2.65	0 ~ 31.3	47
Blue	0 ~ 3.11	0 ~ 30.9	33
Violet	0 ~ 3.31	0 ~ 25.3	33

Tab. 1. Actual data in the circuit measured by multimeter. It is considered that measure the data via the Analog-to-Digital Converter input of Arduino Mega 2560. Range of Voltage refers to the voltage across the LED. Range of Current refers to the current across the LED. Matching Resistor refers to the resistor added between the emitter with ground.

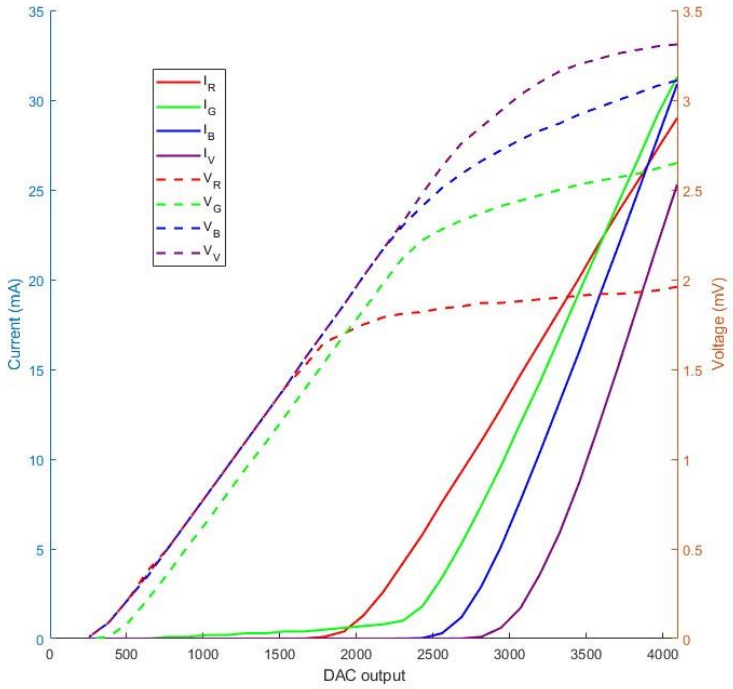

Fig. 5. Actual data in the circuit measured by multimeter. The solid line represents the currents, and the dotted line represents the voltage. The *x*-axis represents the value of DAC output which is from 0 to 4095 (represents the actual output voltage from 0 to 5 V). The left *y*-axis is the current and the right *y*-axis is the voltage.

To better blend the light sources of different color LEDs, we placed a translucent plastic cover with white coating directly above the LED group. The white particles or coating help scatter the light emitted by the LEDs, making it more uniform and preventing the occurrence of glaring light spots or areas with excessive brightness. Additionally, the cover helps to weaken the narrow spectral characteristics of individual LEDs, allowing for better spatial mixing of the light colors from different LEDs, resulting in a more continuous and smooth color effect. This design plays a crucial role in enhancing visual comfort and color uniformity. The following shows the light blending effect achieved with the white translucent cover (it did not work perfectly and we are still looking for better mixer).

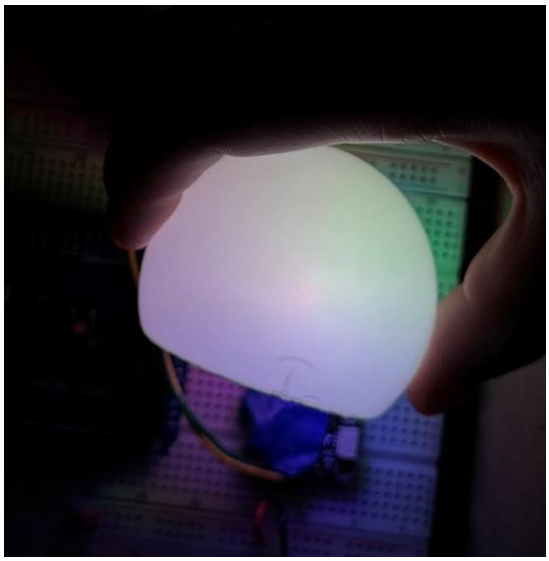

Fig. 6. Using translucent plastic balls to combine with RGB LED light sources to create white.

To further verify the theory and modeling, we designed a method to simulate violet LED light using RGB primary color sources. If the RGB combination can closely simulate the color emitted by the violet LED, it would suggest that adding the violet LED to the experiment might be unnecessary. However, if it cannot be simulated, this would indicate that the experimental design is reasonable. Currently, we have yet to establish a rigorous experimental scheme and metrics for quantifying the similarity between the two colors. It is considered that use an AS7341 10-Channel Light/Color Sensor to compare the 2 colors in the future. Therefore, we searched for possible simulations and visually compared the results, but no RGB combination was found that could simulate the color of the violet LED. Due to the inherent limitations of current displays, it is impossible to accurately display the real color of the violet LED for comparison in the form of an image, so no images are included here.

Method

Brightness Normalization

To facilitate comparison and color gamut size comparison, brightness and chromaticity are separated in this study. For light source *i*, the sum of the responses of the three types of cone cells, $L_i + M_i + S_i$, is considered the brightness, while the ratio of the responses of the three cone cells represents chromaticity. For example, (0.3, 0.1, 0.8) and (0.7, 0.2, 0.3) have the same brightness (since the sum of the three cone responses is 1.2), while (0.2, 0.4, 0.8) and (0.1, 0.2,

0.4) have the same chromaticity (since the ratio of the three cone responses is 1: 2: 4). In this project, we normalize brightness to 1 and only consider the chromaticity, i.e.,

$$\begin{cases} l_i = \dfrac{L_i}{L_i + M_i + S_i} \\ m_i = \dfrac{M_i}{L_i + M_i + S_i} \\ s_i = \dfrac{S_i}{L_i + M_i + S_i} \end{cases} \tag{1}$$

in which l_i, m_i, s_i are the response values of the three types of cone cells to light source *i* after brightness normalization.

Additive Color Theory

According to the additive color theory [23], when n light sources are combined, the response values of the three types of cone cells are the sum of the response values of the corresponding cones for each individual light. That is,

$$\begin{cases} L = \sum_{i=1}^{n} L_i I_i \\ M = \sum_{i=1}^{n} M_i I_i \\ S = \sum_{i=1}^{n} S_i I_i \end{cases} \tag{2}$$

in which, I_i is the relative intensity of light source *i*.

Visual Cone Sensitivity

In this project, we directly used the research results from Colour & Vision Research Laboratory (CVRL) database [24]. CVRL provides the sensitivity of LMS to monochromatic light wavelengths ranging from 390.0 nm to 830.0 nm with a step size of 0.1 nm, and their experiments will be mentioned below briefly. To ensure data reliability, we removed the controversial data at 390-400 nm and 700-830 nm, which means we restrict ourselves to 400-700 nm.

S-cones test [11]: The primary experimental subjects were normal vision humans and S-cone monochromats (individuals with defective M and L cones). The subjects observe a background light, primarily consisting of fixed-intensity long-wavelength light, with a variable intensity and wavelength light point (target light) superimposed on it. The intensity of the target light is adjusted until the subject can just perceive it, and the corresponding light intensity is recorded as the threshold intensity. The threshold intensity is the inverse of sensitivity, and normalization gives the S-cone sensitivity.

M-cones & L-cones test [12]: The sensitivity of M and L cones was tested similarly using TSM, but separating the effects of the other cones is challenging. In this experiment, because S-cones are not sensitive to certain frequencies of flickering light, a flickering target light at a specific frequency was used to minimize the influence of S-cones. Due to the high overlap in wavelength sensitivity between M and L cones, it was difficult to test these cones individually. The experiment relied on two groups of participants: protanopes (L-cone defective) and deuteranopes (M-cone defective). Through these two special types of subjects, and minimizing the influence of S-cones, the sensitivity data for both cones could be obtained by the same attempt of S-cones test.

LED Cone Response

Due to the manufacturing process, the LED light sources are discrete, narrow-band spectral emitters, so we cannot directly obtain the corresponding human three-cone cell response values from the database mentioned earlier. Based on the principle of additive color mixing, we applied a calculus-based method, using a Gaussian distribution and a half-bandwidth of 20 nm, with an integration step size of 0.1 nm, to calculate the corresponding human three-cone cell response values for each LED light source.

$$\begin{cases} L_{LED} = \int_{\lambda_1}^{\lambda_2} L(\lambda) I(\lambda) d\lambda \\ M_{LED} = \int_{\lambda_1}^{\lambda_2} M(\lambda) I(\lambda) d\lambda \\ S_{LED} = \int_{\lambda_1}^{\lambda_2} S(\lambda) I(\lambda) d\lambda \end{cases} \tag{3}$$

In which, $I(\lambda)$ is the relative luminous intensity function of LED. In actual calculations, we take $d\lambda$ as 0.1 nm, λ_1 and λ_2 are taken at three half-bandwidths to the left and right of the main wavelength respectively.

	Dominant wavelength (nm)	Half bandwidth (nm)
Red	640	20
Green	520	20
Blue	465	20
Violet	400	20

Tab. 2. Data used in the theoretical calculation part.

It can be calculated that under normalized brightness, the three cone cell response values of RGB and violet LEDs are

	l	***m***	***s***
Red	0.8485	0.1515	0
Green	0.4278	0.5330	0.0392
Blue	0.1065	0.1783	0.7151
Violet	0.0339	0.0411	0.9250

Tab. 3. Under brightness normalization, the three cone cell response values of the RGB and violet LEDs were used in the experiment.

Color Gamut

According to the principle of additive color mixing and simple linear algebra, we know that under normalized brightness (in the [1, 1, 1] plane), all the colors formed by any combination of light sources are represented by the convex polygonal shape enclosed by these sources in the plane (Fig. 2). For example, the RGB color gamut forms a triangle, the four-color LED gamut forms a quadrilateral, and the visible color gamut is the area enclosed by all visible monochromatic light.

$$\begin{cases} l = \frac{\sum_{i=1}^{n} l_i I_i}{I} \\ m = \frac{\sum_{i=1}^{n} m_i I_i}{I} \\ s = \frac{\sum_{i=1}^{n} s_i I_i}{I} \end{cases} \tag{4}$$

In which,

$$I = \sum_{i=1}^{n} I_i \text{ and } I_i > 0$$

Thus,

$$l + m + s = \frac{\sum_{i=1}^{n} (l_i + m_i + s_i) I_i}{I} = 1 \tag{5}$$

Coloring

To display the color gamut more intuitively, we find different sRGB values for the responses of different cone cells and color the corresponding points. We convert LMS to sRGB values through matrix transformations [10] from CIE standards.

$$\begin{bmatrix} X \\ Y \\ Z \end{bmatrix} = \begin{bmatrix} 1.91020 & -1.11212 & 0.20191 \\ 0.37095 & 0.62805 & 0.00000 \\ 0.00000 & 0.00000 & 1.00000 \end{bmatrix} \begin{bmatrix} L \\ M \\ S \end{bmatrix} \tag{6}$$

$$\begin{bmatrix} X \\ Y \\ Z \end{bmatrix} = \begin{bmatrix} 0.49000 & 0.31000 & 0.20000 \\ 0.17697 & 0.81240 & 0.01063 \\ 0.00000 & 0.01000 & 0.99000 \end{bmatrix} \begin{bmatrix} R \\ G \\ B \end{bmatrix} \tag{7}$$

Finally, the RGB values usually need to be clipped so that the results fall within the range [0, 1]. Specifically, we set the value of R, G, or B to 0 if it is less than 0 and to 1 if it is greater than 1.

NPN Transmitter

The NPN transistor is composed of three layers of semiconductor device: the emitter (E), base (B), and collector (C) [22]. In an NPN transistor, current flows from E, is regulated through B, and then exits through C. Specifically:

- The B-E junction is a PN junction, which typically requires a forward voltage to allow the current to flow from the base into the emitter.
- The B-C junction is a PN junction, where the collector current flows into the base.

When a small current flows from B to E, it causes a large current to flow from C to B, thereby generating a larger current to E. The ratio of C current to B current is usually referred to as the transmitter's current gain (β) typically ranging from tens to hundreds, which is 250 in the NPN we are using. The relationship among the currents over B, C, and E can be expressed by the following equation:

$$I_C = \beta I_B \tag{7}$$

$$I_E = I_B + I_C \approx I_C \tag{8}$$

In which, I_C is the collector current, I_B is the base current, I_E is the emitter current, and β is the current amplification factor of the transmitter.

Conclusion

This project demonstrates that sRGB LED displays significantly fall short of the full color gamut perceivable by the human eye, covering only about 52%. By introducing a fourth principal color, 400 nm violet LED, we achieved approximately 38% progress over sRGB LED, about 72% of visible gamut.

Theoretical calculations revealed that violet light is particularly effective in expanding the color gamut, especially within the violet spectral range. In applications, the project developed a practical circuit system, including RGBV LEDs, DAC, NPN transistors, and a translucent white coating, to ensure precise brightness control and LED light fusion.

This project demonstrates the potential of a four-principal-color LED system for improved color reproduction, which may be useful for practical applications such as medical imaging, design, art restoration, and display technology.

Prospect

In the theoretical part, future research could explore the inclusion of additional wavelengths of LEDs to further expand the color gamut and optimize these findings for practical applications. Specifically, we plan to add a fifth or even a sixth LED to fill in the green and deep red regions that are currently unreachable in the four-color LED gamut.

In the application part, although the current experiment has certain subjectivity and limitations, it lays the foundation for future research. Subsequent work will focus on developing quantitative evaluation methods to ensure the scientific validity, objectivity**,** and reproducibility of the experimental results. The next step will be identifying methods in the experiment to demonstrate that the four-color LED combination with violet LED can simulate a richer set of colors than the RGB system. This step will address challenges such as individual physiological differences, color discrepancies between displays, camera settings, and even psychological factors. To be specific,

Reference

[1] Whitaker, R. (1973). "The Invention of Television." McGraw-Hill.

[2] Fisher, D., & Fisher, M. (1996). "Tube: The Invention of Television." Random House.

[3] Schure, A. (1955). "Color Television: Theory and Practice." McGraw-Hill

[4] Stokes, M., Anderson, M., Chandrasekar, S., & Motta, R. (1996). "A Standard Default Color Space for the Internet - sRGB." HP and Microsoft.

[5] Poynton, C. (2003). "Digital Video and HDTV: Algorithms and Interfaces."

[6] Sharma, G. (2003). "Digital Color Imaging Handbook."

[7] Adobe Systems Incorporated. (1998). "Adobe RGB (1998) Color Image Encoding."

[8] Kodak Inc. (1999). "ProPhoto RGB Color Space Specification."

[9] Digital Cinema Initiatives, LLC. (2007). "Digital Cinema System Specification v1.0."

[10] CIE. (1931). "Standard Colorimetric System."

[11] Stockman, A., Sharpe, L., & Fach, C. (1999). "The spectral sensitivity of the human short-wavelength sensitive cones derived from thresholds and color matches." Vision Research.

[12] Stockman, A., & Sharpe, L. (2000). "The spectral sensitivities of the middle- and long-wavelength-sensitive cones derived from measurements in observers of known genotype." Vision Research.

[13] Adafruit. "https://www.adafruit.com/product/297".

[14] Adafruit. "https://www.adafruit.com/product/300".

[15] Adafruit. "https://www.adafruit.com/product/301".

[16] Adafruit. "https://www.adafruit.com/product/1793".

[17] Arduino.cc. "https://store.arduino.cc/products/arduino-mega-2560-rev3".

[18] Adafruit. "https://www.adafruit.com/product/4470".

[21] Bhattacharya, P. (1997). "Semiconductor Optoelectronic Devices." Prentice Hall.

[22] Sze, S. M. (2002). "Semiconductor Devices: Physics and Technology." John Wiley & Sons.

[23] Berns, R. S. (2000). "Principles of Color Technology." John Wiley & Sons.

[24] CVRL. "http://cvrl.ucl.ac.uk".

Supplement

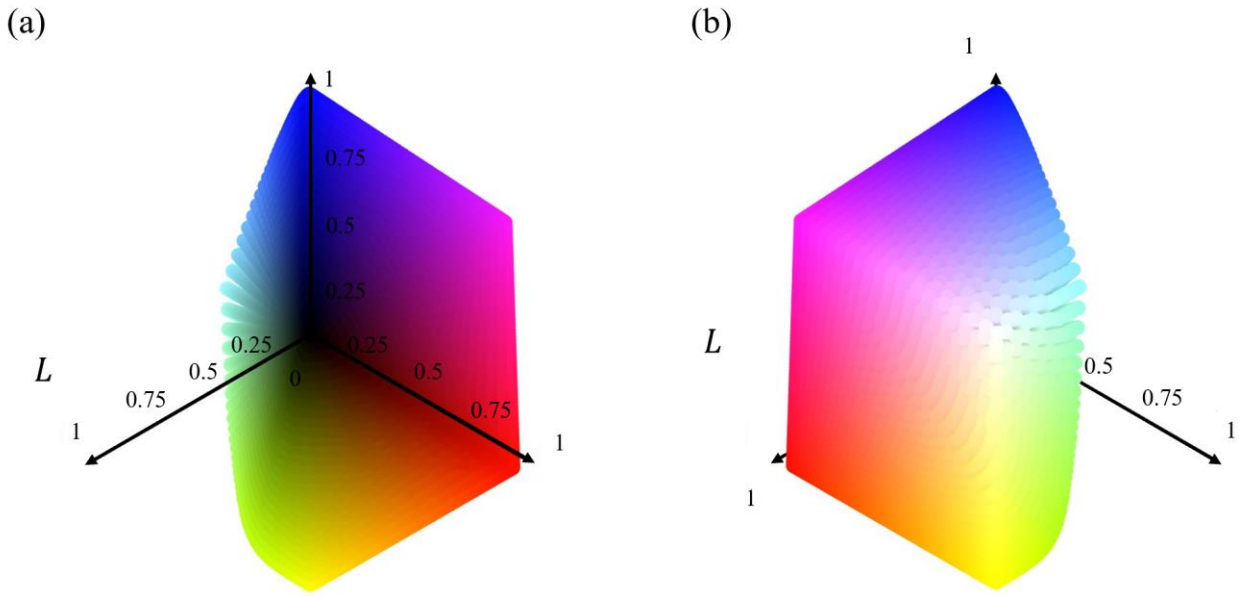

Fig. S1. Different views of three-dimensional human-visible color gamut. (a) the view from direction [-1, -1, -1] and (b) the view from direction [1, 1, 1].